Attenuation and Dispersion for High-T_c Superconducting Microstrip Lines

ERIK B. EKHOLM AND STEPHEN W. MCKNIGHT, MEMBER, IEEE

Abstract—**We have calculated the attenuation and dispersion of microstrip lines of the high-T_c superconductor $YBa_2Cu_3O_7$ (YBCO) on yttria-stabilized zirconia (YSZ) substrates as a function of frequency and temperature. YBCO is modeled as a BCS superconductor with a critical temperature $T_c = 90$ K and a superconducting energy gap $2\Delta = 4.5kT_c$. The effect on pulse propagation of superconducting and modal dispersion in addition to the attenuation is demonstrated. At 60 K, microstrip lines of YBCO are significantly less attenuating at frequencies below 500 GHz than microstrip lines of copper at the same temperature. This advantage is particularly significant at the higher attenuations that result as the substrate thickness is made smaller for miniaturization or to improve the microstrip line bandwidth. The application of YBCO for microstrip lines appears to be most useful at frequencies above 100 GHz and dielectric thicknesses less than 100 μm, where the attenuation of cooled copper is prohibitively large. Cooled to temperatures below 20 K, YBCO may make possible a new generation of extremely high bandwidth (~ 5 THz), small feature size (~ 5 μm) circuits and devices.**

I. INTRODUCTION

AMONG THE most promising applications foreseen for the new high-T_c superconductors is in the fabrication of high-frequency devices. Superconductors are known to have extremely low surface resistance, and can be used to make transmission line devices featuring extremely low losses and low signal distortion. The discovery of the high-T_c materials may make these advantages available at relatively high temperatures. They may also extend the low-distortion frequency range into the terahertz range.

Examination of a stripline with the old "low-T_c" superconductors has been done by Kautz [1]. In his analysis he did not include the modal dispersion, which will be shown later to have a serious impact on the transmission line performance. Whitaker *et al.* [2], [3] have included the effects of modal dispersion in a coplanar waveguide. The effect of the new high-T_c superconductors on the dispersion and attenuation of a stripline has been considered in the two-fluid model by Kwon *et al.* [4]. Experimentally, Dykaar *et al.* [5] have fabricated transmission lines of the high-T_c superconductor $YBa_2Cu_3O_7$ and compared their properties with BCS calculations. The transmission of picosecond pulses in a coplanar waveguide structure was found to show very low distortion.

Manuscript received August 17, 1989; revised November 13, 1989.

E. B. Ekholm is with the Center for Electromagnetics Research, Northeastern University, Boston, MA 02155, and with the Royal Institute of Technology, Stockholm, Sweden.

S. W. McKnight is with the Center for Electromagnetics Research, Northeastern University, Boston, MA 02115.

IEEE Log Number 8933713.

In this paper we will calculate the attenuation and phase velocity for microstrip transmission lines constructed of the high-T_c superconductor $YBa_2Cu_3O_7$ (YBCO) as a function of frequency and temperature. The effects of substrate material will be examined, and common YBCO substrates evaluated. Modal dispersion and attenuation due to losses in the superconductor will be calculated, and the effect on pulse propagation illustrated. We will compare these results with what can be obtained with copper microstrip lines operating at 60 K. Frequency and temperature regions where significant advantage can be obtained with YBCO will be highlighted.

II. SUBSTRATE EFFECTS

High-quality YBCO films were first achieved on $SrTiO_3$ substrates, but $SrTiO_3$, with its large, temperature-dependent dielectric constant ($\epsilon_r \sim 1900$ at 77 K, $d\epsilon/dT \sim -35$ K^{-1}), is unsuitable for microstrip line applications. We have investigated several other possible substrate materials and considered their suitability for microstrip lines. The results are given in Table I, which tabulates the dielectric constant for microwave frequencies at 80 K. We have also calculated the stripline width to substrate thickness ratio (W/h in Fig. 1) for a 50 Ω stripline and the attenuation due to conductivity losses in the metallic strip and ground plane. For this last calculation we have assumed a copper microstrip and ground plane at 60 K, a frequency of 10 GHz, and a dielectric thickness of 0.5 mm. Dielectric losses at low temperatures, calculated from the loss tangent values given in the table, are less than the conductivity losses for all these substratematerials except $SrTiO_3$. Low-conductivity-loss superconducting microstrip lines, therefore, could be a great advantage in terms of system transmission and heat load. We have also indicated in the table the cutoff frequency where multimode transmission becomes possible. At frequencies above f_c the microstrip line supports a variety of waveguide modes as well as the quasi-TEM mode of low frequencies. This will result in a dispersion of the signal phase velocity and pulse-shape distortion. This modal dispersion will be considered in detail below.

At present, reproducible high-quality YBCO films are being produced on cubic zirconia (YSZ) substrates as well as $SrTiO_3$. Although the dielectric constant of YSZ is still not ideal, we will make our calculations in the remainder

0018-9480/90/0400-0387$01.00

TABLE I
MICROSTRIP LINE SUBSTRATE MATERIALS

Material	ϵ_r	Z_0 (Ω)	W/h	$\tan\delta$	α_c (dB/m)	f_c (GHz)	Ref.
CaF_2	6.49	50	1.4	$2\cdot10^{-4}$	1.1	64.0	[6]
Al_2O_3*	8.30	50	1.1	$1\cdot10^{-6}$	1.3	55.0	[7]–[9]
MgO	9.65	50	0.94	$4\cdot10^{-4}$	1.5	51.0	[6]
Cr_2O_3	12.8	50	0.70	$1\cdot10^{-3}$	1 9	44.0	[10]
ZrO_2 : Y**	27.0	50	0.24	$6\cdot10^{-4}$	4.4	29.0	[11], [12]
$SrTiO_3$***	1875.0	3.6	1.0	10^2	20.0	3.6	[13]–[15]

*Averaged over crystallographic orientations.
**Yttria-stabilized cubic zirconia (YSZ).
***W/h unphysically small for $Z_0 = 50\ \Omega$, calculated for $W/h = 1.0$.
The table shows the dielectric constant at microwave frequencies and 80 K (YSZ at 4.2 K) for $YBa_2Cu_3O_7$ substrate materials. Also shown are the microstrip width/separation ratio W/h for a 50 Ω characteristic impedance, the conductivity attenuation α_c and cutoff frequency f_c calculated for dielectric separation $h = 0.5$ mm and conductor thickness $t = 0.01$ mm. The surface resistance is taken to be $R_s = 0.0083\ \Omega$, appropriate for copper at 60 K and 10 GHz.

of the paper assuming a YSZ substrate 500 μm thick. Higher cutoff frequencies could be achieved with thinner substrates and lower dielectric constants. The results can be scaled to different substrates and geometries as the limits of the high-T_c technology become clearer. Other substrate materials include magnesium oxide (MgO) and lanthanum gallate [16].

YBCO is assumed to be a BCS-type superconductor, with a T_c of 90 K and a superconducting energy gap at $T = 0$, $2\Delta(0)$, of 35 meV. Whether the new superconductors can in fact be described by the BCS theory, and indeed whether they have any energy gap at all, are still subjects of controversy. It is clear that bulk ceramic samples have microwave surface impedances orders of magnitude higher than predicted by BCS theory [17]. The response of these materials is believed to be dominated by Josephson junctions at the grain boundaries. In the best single crystals and oriented *ab*-plane materials, however, surface impedances below 10^{-4} Ω have been measured—approaching the BCS limit [18]. Gaplike behavior has been observed in far-infrared experiments on films of oxygen-depleted YBCO [19], and recent measurements of the gap energy have given values for the ratio $2\Delta/kT_c$ very near the BCS weak coupling value of 3.54 [20]. The question of whether BCS theory will describe the superconducting behavior of the new materials may not be resolved for many years. Nevertheless, it is of interest to apply BCS theory to high-T_c devices for two reasons: 1) any theory which predicts an energy gap at the Fermi level will have many of the same features in the frequency-dependent conductivity as BCS theory, and 2) BCS theory is the only available basis we have for calculation. It is important to establish a reference point for interpreting experimental results and to predict limits on device performance. The ability to reach these limits will depend on the fundamental limits of superconductivity in these materials and on the progress of materials science in producing high-quality, low-surface-impedance films.

With these considerations in mind, we have made our calculations assuming the observed critical temperature and a value of the gap which yields $2\Delta/kT_c = 4.5$. This value is in the middle of the range indicated by infrared measurements available at this time [20]. The structure of the microstrip line is shown in Fig. 1 and the parameters of our calculation are summarized in Table II. We will be comparing our results with the performance of a copper microstrip line. The dc resistivity of copper is about 0.2 $\mu\Omega\cdot$cm at 60 K and the surface resistance is assumed to be given by the classical formula

$$R_s = (\pi f \mu_0 \rho)^{1/2}. \tag{1}$$

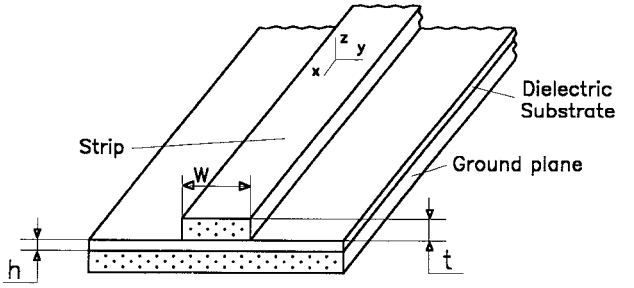

Fig. 1. Geometry and nomenclature for microstrip line.

TABLE II
MICROSTRIP MODELING PARAMETERS

	Strip	Dielectric Substrate
Material	YBCO	Cubic zirconia (YSZ)
Thickness	0.05 mm	0.5 mm
Width	0.5 mm	
ϵ_r		27.0
$2\Delta(0)$	35 meV	
T_c	90 K	

III. MICROSTRIP THEORY

The propagation of a sinusoidal voltage $V(x,\omega)e^{j\omega t}$ on a transmission line is governed by the following differential equation:

$$\frac{d^2V}{dx^2} = \gamma^2 V \tag{2}$$

where γ is the propagation constant. By using the series impedance Z and the shunt admittance Y, γ can be approximated by

$$\gamma = [ZY]^{1/2} = \frac{Z}{Z_0} \tag{3}$$

where Z_0 is the characteristic impedance. The propagation constant can be divided into its real and imaginary parts:

$$\gamma = \alpha + j\beta \tag{4}$$

where the real part, α, is commonly understood as the attenuation and the imaginary part, β, as the phase factor.

The attenuation is affected by conductor and dielectric losses; the phase factor is mainly influenced by the line geometry but also to some extent by the conductor. It is therefore convenient to divide α and β into two parts:

$$\alpha = \alpha_c + \alpha_d$$
$$\beta = \beta_c + \beta_m. \tag{5}$$

For the microstrip the series impedance and the shunt admittance are given by

$$Z = j\omega\mu_0 g_1 + 2Z_s g_2 \tag{6}$$

$$Y = \omega\epsilon_0\left(j\epsilon_r^{\text{eff}} + \epsilon_r \tan\delta\right)/g_1 \tag{7}$$

where μ_0 is the permeability of free space (the dielectric is assumed to be nonmagnetic), Z_s is the complex surface impedance, ϵ_0 is the permittivity of free space, ϵ_r^{eff} is the effective dielectric constant, ϵ_r is the relative permittivity of the substrate, $\tan\delta$ is the loss tangent of the substrate, and g_1 and g_2 are functions depending on the geometry of the line. Expressions for g_1 and g_2 are given in [21] and [22]. Although all calculations have been performed on a microstrip, the results are valid on other transmission line structures merely by adjusting g_1 and g_2 to the geometry of the line.

IV. Evaluation of the Propagation Constant

This section describes a method to calculate the four parts of the propagation constant γ as described by equations (5).

A. Superconducting Loss

The distinguishing characteristic of a superconductor is the energy gap separating the ground state from the lowest excited state for the superconducting electrons. A superconducting stripline will feature low transmission losses up to the frequency corresponding to the energy gap:

$$f_{\text{gap}} = \frac{2\Delta(T)}{\hbar 2\pi}. \tag{8}$$

The energy gap $2\Delta(T)$ can be calculated from the expression given in [24]. The energy gap is shown in Fig. 2 for YBCO, which has $T_c \approx 90$ K and $2\Delta(0) \approx 4.5kT_c \approx 35$ meV.

The attenuation in a microstrip depends on the characteristic impedance Z_0 of the transmission line and on the surface resistivity of the ground plane and the strip. Using (3), the attenuation due to the superconductors can be written as

$$\alpha_c = \text{Real}\left\{\frac{Z_s}{Z_0}\right\} g_2 \qquad (\text{m}^{-1}) \tag{9}$$

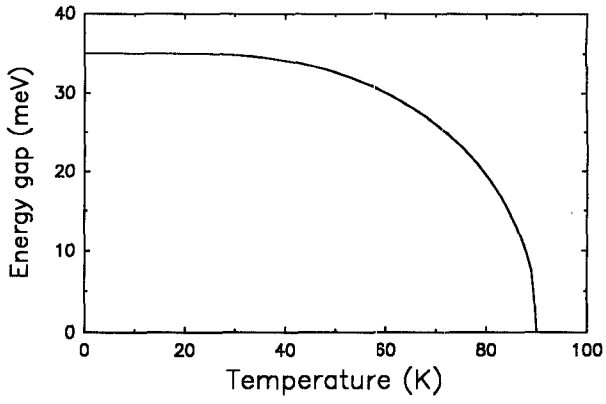

Fig. 2. Calculated temperature dependence of the superconducting energy gap for YBCO.

where Z_s is the surface impedance of the conductors, assuming the ground plane and the strip are of the same material.

In the extreme local limit the surface impedance of a superconductor is given by Ginsburg [23]:

$$Z_s(f) = (1+j)\left[\frac{\omega\mu_0}{2\sigma_n}\right]^{1/2}\left[\frac{\sigma_1 - j\sigma_2}{\sigma_n}\right]^{-1/2} \tag{10}$$

where σ_n is the normal state conductivity, and σ_1 and σ_2 are the real and imaginary parts of the complex conductivity of a superconductor. For YBCO we take σ_n to be 100 $\mu\Omega\cdot$cm, the value just above T_c.

Mattis and Bardeen [25] have derived expressions for σ_1 and σ_2 using the BCS weak-coupling theory:

$$\frac{\sigma_1}{\sigma_n} = \frac{2}{\hbar\omega}\int_{\Delta}^{\infty}[f(\epsilon) - f(\epsilon+\hbar\omega)] \times \frac{\epsilon^2 + \Delta^2 + \hbar\omega\epsilon}{(\epsilon^2-\Delta^2)^{1/2}\left[(\epsilon+\hbar\omega)^2-\Delta^2\right]^{1/2}}\,d\epsilon + \frac{1}{\hbar\omega}\int_{\Delta}^{\hbar\omega-\Delta}[1-2f(\hbar\omega-\epsilon)] \times \frac{\hbar\omega\epsilon - \epsilon^2 - \Delta^2}{(\epsilon^2-\Delta^2)^{1/2}\left[(\hbar\omega-\epsilon)^2-\Delta^2\right]^{1/2}}\,d\epsilon \tag{11}$$

$$\frac{\sigma_2}{\sigma_n} = \frac{1}{\hbar\omega}\int_{\Delta-\hbar\omega,-\Delta}^{\Delta}[1-2f(\epsilon+\hbar\omega)] \times \frac{\epsilon^2 + \Delta^2 + \hbar\omega\epsilon}{(\epsilon^2-\Delta^2)^{1/2}\left[(\hbar\omega+\epsilon)^2-\Delta^2\right]^{1/2}}\,d\epsilon \tag{12}$$

where $\Delta = \Delta(T)$, $\omega = 2\pi f$, σ_n is the normal state conductivity of the superconductor, and $f(\epsilon)$ is the Fermi function.

The first integral of σ_1 represents conduction by thermally excited normal electrons, while the second integral, which is zero for $\hbar\omega < 2\Delta$ (or for frequencies below f_{gap}),

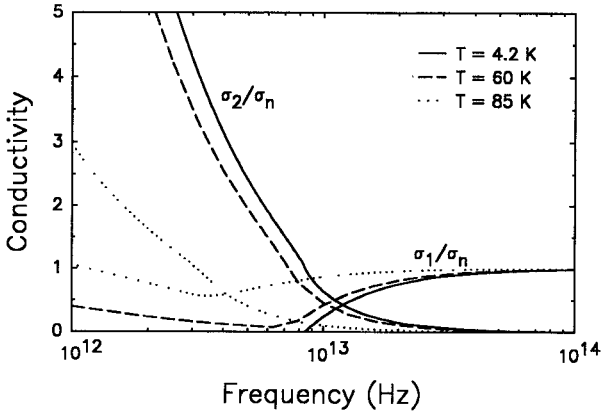

Fig. 3. Complex conductivity for YBCO ($f_{gap} = 8.5$ THz).

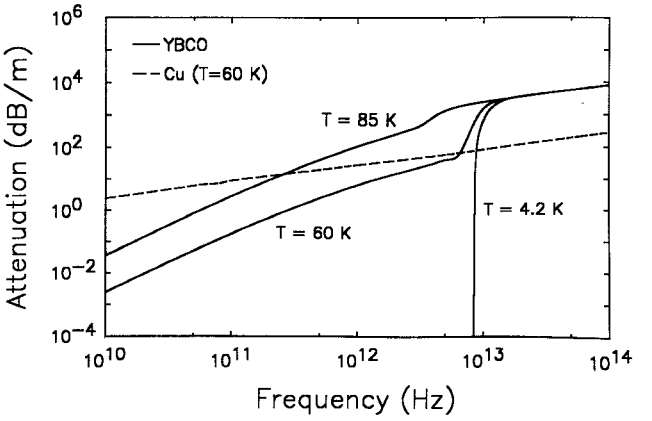

Fig. 4. Attenuation as a function of frequency for microstrip line with YSZ substrate, $h = 500$ μm. Note that attenuation scales with $1/h$.

represents the generation of quasi-static particles due to pair-breaking by high-frequency fields. The quantity σ_2 describes the superconducting electrons. The lower limit on the integral for σ_2 describes the superconducting electrons. The lower limit on the integral for σ_2 becomes $-\Delta$ when $\hbar\omega > 2\Delta$. Equations (11) and (12) are shown in Fig. 3 for YBCO.

In Fig. 3 we can also see the effect of the temperature dependence on the gap energy. The sharp rise in σ_1/σ_n at $T = 4.2$ K occurs at the frequency corresponding to the energy gap, $f_{gap} \approx 8.5$ THz. The missing area under the σ_1/σ_n curve is compensated for by a delta function at $f = 0$ (infinite dc conductivity), as required by sum rules [26]. At higher temperatures, the onset of the increase in σ_1 moves to lower frequencies and absorption near $f = 0$ appears due to the spreading of the delta function.

For the microstrip described in Table II the attenuation as a function of frequency and temperature is shown in Fig. 4 and Fig. 5. Data for copper at 60 K and 24 GHz are shown for comparison [27]. In Fig. 4 we can see that the attenuation for YBCO depends strongly on the frequency, with a sharp rise at f_{gap}.

From this analysis we can realize that it is necessary to operate the microstrip at temperatures much lower than the critical temperature, T_c, and avoid signals with a frequency content close to and above the gap frequency.

B. Dielectric Loss

When the dielectric substrate filling the region between conductors in a transmission line is lossy,

$$\alpha_d = \text{Real}\{\gamma\} \approx \pi \frac{\epsilon_r \tan\delta}{\sqrt{\epsilon_r^{\text{eff}}}} \frac{1}{\lambda_0} \quad (\text{m}^{-1}) \qquad (13)$$

where λ_0 is the free-space wavelength.

We can see that the line geometry has slight impact on the dielectric loss. For small dielectric spacing, attenuation due to the dielectric substrate is much less than attenuation due to the conductors. Further studies of the dielectric losses have been done by Pucel *et al.* [28]. In the further treatment, the contribution by dielectric loss to γ is neglected.

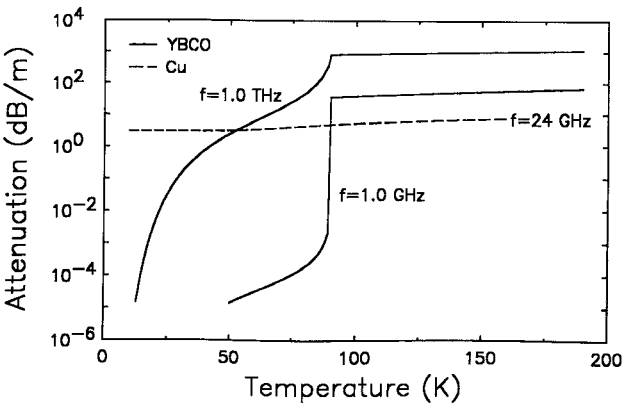

Fig. 5. Attenuation as a function of temperature for microstrip line on YSZ substrate.

C. Superconducting Dispersion

The expression for the superconducting dispersion is of the same type as (8):

$$\beta_c = \text{Im}\left\{\frac{Z_s}{Z_0}\right\} g_2 \quad (\text{m}^{-1}) \qquad (14)$$

where Z_s is given by (9).

By (5), the imaginary contribution due to conductors, β_c, adds to the modal phase factor β_m in order to give the full phase factor, $\beta(f)$, for the signal. Even with the large variation in β_c due to the change in conductivity around f_{gap}, the impact of the dispersion due to the superconductor on the full phase factor is less than 0.1%. Therefore, it is usually not necessary to include β_c in the analysis of the propagation constant and only the real part of Z_s needs to be considered.

D. Modal Dispersion

The microstrip is inherently dispersive—it is incapable of supporting a pure TEM wave except at zero frequency. The reason is that a TEM wave requires that

$$\gamma^2 + k^2 = 0 \qquad (15)$$

where k is the wavenumber and the propagation constant γ is a single constant for the line. The microstrip has a dielectric substrate between the strip and the ground plane

and a different dielectric substrate, usually air, above the insulator and the strip (see Fig. 1). Therefore $\gamma^2 + k_1^2$ and $\gamma^2 + k_2^2$ cannot both be zero when $k_1 \neq k_2$ (k_1 and k_2 are the wavenumbers in the dielectric and air respectively). An approximate approach is to consider the lowest order wave to be approximately a TEM wave so the distribution of fields in the transverse plane is the same as that for static fields. A low-frequency effective dielectric constant ϵ_r^* can then be calculated [21], [22], [29].

For the parameters of our microstrip line ($W = h \gg t$) we find

$$\epsilon_r^* = \frac{\epsilon_r + 1}{2} + \frac{\epsilon_r - 1}{2\sqrt{13}}. \tag{16}$$

The effective dielectric constant can be approximated by (16) only up to the cutoff frequency, defined as

$$f_c = \frac{c}{4h\sqrt{\epsilon_r - 1}}. \tag{17}$$

Equation (17) gives the region in which the first longitudinal mode—TE_1 for a microstrip—contributes significantly. For the stripline given in Table II, $f_c \approx 28$ GHz.

Dispersion at high frequencies has been analyzed by several authors using different techniques to find the frequency-dependent effective dielectric constant ϵ_r^{eff} [30]–[38]. All these analyses yield a low-frequency effective dielectric as given by (16), a transition band around f_c, and above the transition band the ϵ_r^{eff} approaches ϵ_r as the transmission line behaves as a waveguide with the wave completely confined to the dielectric region. We have used the numerical approximation of Yamashita *et al.* [31] to find $\epsilon_r^{\text{eff}}(f)$. The modal phase factor is given by

$$\beta_m = \frac{2\pi f}{c}\sqrt{\epsilon_r^{\text{eff}}(f)} \qquad (\text{m}^{-1}). \tag{18}$$

The propagation velocity of a signal depends on the effective dielectric constant as

$$v_\phi = \frac{2\pi f}{\beta_m + \beta_c} \simeq \frac{c}{\sqrt{\epsilon_r^{\text{eff}}(f)}} \tag{19}$$

where the second equality holds because $\beta_m \gg \beta_c$. The phase velocity is plotted in Fig. 6. The decrease in the phase velocity due to the change in the effective permittivity is observed. If a pulse propagating on the microstrip contains frequency components in the region where the phase velocity varies significantly, severe distortion of the pulse will occur as a result of this function. The effect of the superconducting dispersion ($\beta_c(f)$) cannot be resolved in the figure.

The transition from higher to lower velocities takes place in the region where the wavelength in the substrate is of the same order as the transverse dimensions of the microstrip. For the microstrip considered, the transition region lies much lower than the frequency corresponding to the energy gap, f_{gap}. We note that the dispersion is primarily due to geometry-dependent modal effects—redistribution of energy from the TEM mode to higher order modes

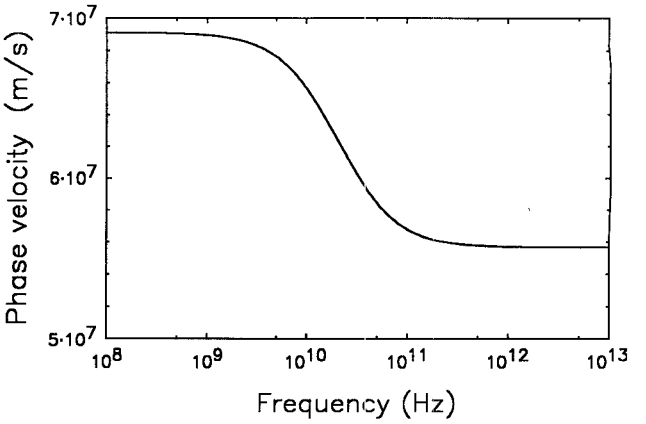

Fig. 6. Phase velocity as a function of frequency for the microstrip given in Table I.

—while the attenuation in this system is almost entirely determined by the completely different physical effects of the stripline conductivity.

V. Pulse Propagation

All of the pieces are now available to calculate the full expression for the propagation factor $\gamma(f)$ according to (4) and (5). This enables us to simulate the propagation of different waves on a transmission line device.

The propagation constant is a function of frequency; thus different spectral components will travel at different velocities and will be attenuated differently. To show the frequency dependence, consider a pulse which is given at $x = 0$ as

$$v(0,t) = \begin{cases} 1, & |t| \leq \dfrac{T_1}{2} \\ 0, & \text{elsewhere.} \end{cases} \tag{20}$$

To obtain the spectral components of the voltage pulse, we take the Fourier transform to obtain the well-known result:

$$V(0,\omega) = \frac{2}{\omega}\sin\frac{T_1}{2}\omega. \tag{21}$$

The signal given by (20) has an infinite spectrum according to (21); i.e., the signal is not band limited, but the effects of distortion—due to attenuation in the conductors and the modal dispersion—are easily shown.

Assuming the line has an infinite extent or is terminated properly to get no reflections, we can calculate the voltage wave after traveling a distance L by solving (1) as

$$V(L,\omega) = V(0,\omega)e^{-\gamma(\omega)L}. \tag{22}$$

Use the inverse Fourier transform to get the voltage pulse after propagating a distance L as

$$V(L,t) = \frac{2}{\pi}\int_0^{-\infty} e^{-\alpha L}\cos(\omega t - \beta L)\frac{1}{\omega}\sin\frac{T_1}{2}\omega\, d\omega \tag{23}$$

after making use of the symmetry of the spectrum.

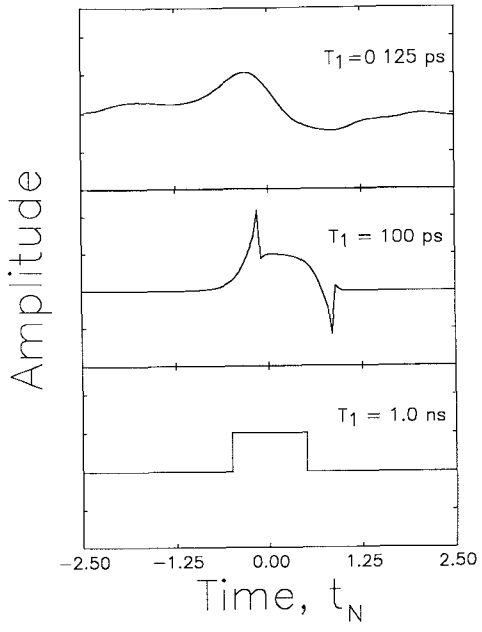

Fig. 7. Pulse shape for a square pulse after propagating a distance $L = 1$ cm for the microstrip given in Table II at $T = 4.2$ K.

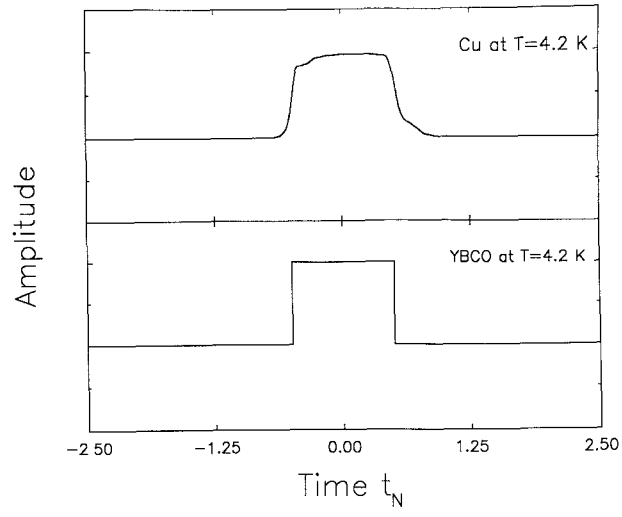

Fig. 8. Pulse shape after propagation for 10 cm on YBCO and copper microstrip lines. Pulse width is $T_1 = 1$ ns

We have evaluated (23) to find the distortion of a pulse propagating on a YBCO microstrip line at 4.2 K. We have used the superconducting attenuation α from Fig. 4 and the dispersion $\beta = \omega/v_\phi$ from the phase velocity in Fig. 6. Fig. 7 shows the pulse after propagating a distance $L = 10$ mm for three different pulse widths. For each trace the origin has been shifted by an amount.

$$t_L = \frac{L}{v_\phi(\omega = 0)} \tag{24}$$

so a pulse composed entirely of low frequencies would be centered at the time origin. To make comparisons easy, the time axis is normalized by

$$t_N = \frac{t - t_L}{T_1}. \tag{25}$$

In Fig. 7 (bottom) $T_1 = 1.0$ ns. This pulse has most of its energy at low frequencies, well below the cutoff frequency. Since the attenuation is less than 10^{-5} dB/m at this frequency and temperature, the pulse is not distorted at all. The line is a perfect device. The lack of dispersion of a YBCO superconducting transmission line at frequencies as high as hundreds of gigahertz has been experimentally demonstrated by Dykaar *et al.* [5]. The measurements were made using a coplanar stripline, which features lower modal dispersion than a microstrip.

In Fig. 7 (middle), the effect of the modal dispersion is evident. The pulse width is $T_1 = 100$ ps. The pulse has spectral components both above and below the transition band (see Fig. 6). Although the energy content of the pulse is almost the same as the original pulse at $x = 0$, the shape is completely distorted.

In Fig. 7 (top) we instead see the effect of the dramatic variation in the attenuation around f_{gap} ($T_1 = 0.125$ ps). This pulse has spectral components both above and below f_{gap}. The pulse is severely distorted and consists mainly of a frequency component at frequency $f \approx f_{gap}$. The energy content is also dramatically reduced, even after propagating 10 mm. It should be noted, however, that this distortion occurs at frequencies above several terahertz.

In Fig. 8, the distortionless propagation of a pulse ($T_1 = 1$ ns) on a superconducting stripline at low temperatures is compared to the results for a copper microstrip line operating at 4.2 K. Since the surface impedance of copper increases as $f^{1/2}$, the high-frequency components are selectively damped as shown in the figure. In contrast, the attenuation of the superconductor at low temperatures is less than 10^{-4} dB/m for all frequencies below f_{gap} and the pulse is propagated with no distortion. For a longer propagation length or a smaller dielectric separation h, the advantage of the YBCO microstrip line is more dramatic.

VI. Device Design Considerations

Applications of YBCO microstrip lines will most likely be restricted to those applications where YBCO has a significant advantage over copper microstrip lines operating at low temperatures. At 80 K copper microstrip lines with a dielectric separation of 0.5 mm have an attenuation on the order of 2 dB/m at 10 GHz. If the surface resistance of YBCO is accurately modeled by the BCS calculation and if the full potential of the material can be realized through progress in material fabrication techniques, YBCO microstrip lines could have attenuations two orders of magnitude lower at 80 K (~ 0.02 dB/m). At 60 K, a temperature which could be reached by pumping on liquid nitrogen or thermoelectric cooling below a liquid nitrogen reservoir, YBCO has an attenuation three orders of magnitude better than copper at 10 GHz and maintains a significant advantage to over 100 GHz. These advantages

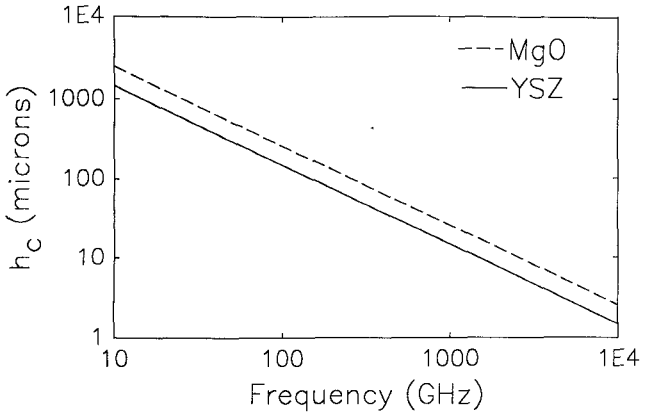

Fig. 9. Cutoff thickness for the propagation of higher order modes on microstrip lines as a function of frequency for MgO and YSG dielectrics.

near liquid nitrogen temperatures may be critical for applications with long propagation lengths or high power. The major area of advantage, however, appears to be the large bandwidths permitted by the low attenuation below 20 K.

To make full use of the extraordinary low-loss bandwidth available with YBCO, it will be necessary to avoid the modal distortion resulting from the relatively low cutoff frequency of the geometry we have considered so far. In the microstrip line geometry this can be done by changing the substrate dielectric constant or by decreasing the substrate thickness. Fig. 9 shows the cutoff frequency as a function of substrate thickness h for a cubic zirconia (YSZ) substrate and also, as an example of a lower dielectric constant substrate, for MgO. To make use of the full 5 THz bandwidth requires dielectric separations of 3 μm (for YSG) or 5 μm (for MgO). These separations could be achieved through a layered structure with the YBCO ground plane grown on a supporting substrate, a 5 μm dielectric layer deposited over the superconductor, and then the stripline patterned on top of the dielectric (Fig. 10).

A decrease in the width of the dielectric will increase the conductivity attenuation proportionally. For a dielectric spacing of 5 μm, for example, the conductivity attenuation of Fig. 4 will be increased two orders of magnitude. At 5 THz this would imply an attenuation in YBCO at 60 K of 3700 dB/m (copper would be even higher) and the device would be unusable. At 4.2 K, however, YBCO would have an attenuation below 10^{-3} dB/m at 5 THz. At this level dielectric attenuation would be the limiting effect. The decrease in the dielectric spacing required for high-frequency (terahertz) dispersionless propagation is only possible due to the low loss of YBCO microstrip at low temperatures. Since the W/h ratio will remain about 1 for characteristic impedances on the order of 50 Ω, the decrease in the dielectric spacing may also make possible circuit miniaturization, with microstrip line widths on the order of 5 μm.

Whether circuit spacing can be made this small will depend on the electromagnetic coupling between adjacent microstrips. This will depend to some extent on the free-

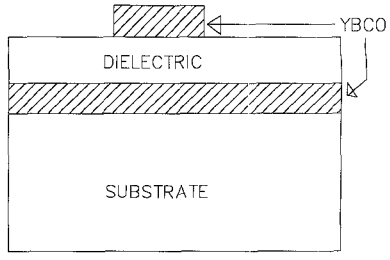

Fig. 10. Sketch of miniaturized microstrip line deposited on supporting substrate for very thin dielectric thicknesses.

space wavelength, but it also seems clear that for smaller dielectric spacing the fields will be concentrated more in the dielectric. Coplanar waveguide, slot line, or enclosed microstrip line geometries may offer some advantages over the open microstrip lines considered here. If it proves feasible to design circuits with stripline spacings in the range of 5 μm, it may make possible a technology of microwave/millimeter-wave/submillimeter-wave circuits with complexity comparable to present integrated circuits. The application of these circuits to analog computing and signal processing could be revolutionary.

The realization of these high-bandwidth, large-scale-integrated millimeter-wave/submillimeter-wave circuits will depend on rapid progress in materials. Both fundamental questions, such as the demonstration of a BCS-like gap in high-T_c materials, and processing problems, such as the technique for depositing low $\tan\delta$ dielectric material compatible with the oxide superconductors, will have to be addressed. In addition, it will be necessary to determine the optimum geometry to reduce feature size and minimize circuit cross talk. Our analysis indicates, however, that the application of high-T_c superconductors to millimeter-wave circuits is an area of great promise.

VII. Conclusion

We have given a systematic method for calculating the full expression for the propagation factor $\gamma(f)$ for a microstrip line fabricated of the high-T_c superconducting YBCO. The effects of the frequency-dependent propagation factor have also been shown.

For the geometry and material parameters given in Table II, the modal dispersion appears at frequencies much lower than the frequency corresponding to the energy gap, f_{gap}. The modal dispersion is due to the transmission line geometry and the choice of dielectric substrate. By making the dielectric substrate thin and/or selecting a dielectric substrate with low relative dielectric constant, the cutoff frequency, and therefore the transition band (see Fig. 6), are raised. We conclude that it is necessary to consider the modal dispersion in the analysis of the transmission line.

At low temperatures, the microstrip with superconducting strip and ground plane features almost lossless transmission up to f_{gap}. This makes the superconducting microstrip superior to one made with ordinary conductors. We have also seen that the effect of the imaginary part of

the surface impedance on the phase velocity can be neglected. This is a useful observation since it is difficult to measure the reactive part of the surface impedance. The impact on the attenuation by the line geometry is small; the major factor is the energy gap. It should also be noted that the microstrip line attenuation is proportional to the surface resistivity of the conductors, so measuring attenuation in the microstrip may be a sensitive way to determine the temperature dependence of the surface resistivity of the superconductor.

The advantage of YBCO microstrip line over normal metal (copper) is most significant for very small dielectric spacing where the conductivity attenuation is greatly increased. Using YBCO at temperatures less than 20 K in place of copper will allow spacing as small as 5 μm with conductivity attenuations less than 10^{-3} dB/m. Since the microstrip line width scales with the spacing this could lead to miniature millimeter-wave circuits. Small spacing also increases the cutoff frequency due to modal effects. For 5 μm spacing the cutoff frequency is on the order of 10 THz, so the microstrip bandwidth extends to the superconducting gap frequency, which is nearly 10 THz. YBCO microstrip lines at low temperatures could thus form the basis of an extremely high bandwidth, large scale integration millimeter-wave/submillimeter-wave technology.

ACKNOWLEDGMENT

The authors are grateful to Prof. W. B. Nowak for the use of his data on the temperature dependence of the surface resistance of copper and to A. I. Braginski for information on substrate materials.

REFERENCES

[1] R. L. Kautz, "Picosecond pulses on superconducting striplines," *J. Appl. Phys.*, vol. 49, pp. 308–314, 1977; "Miniaturization of normal-state and superconducting stripines," *J. Res. Nat. Bur. Stand.*, vol. 84, pp. 247–259, 1979.

[2] J. F. Whitaker, T. B. Norris, G. A. Mourou, and T. Y. Hsiang, "Pulse dispersion and shaping in microstrip lines," *IEEE Trans. Microwave Theory Tech.*, vol. MTT-35, pp. 41–47, 1987.

[3] J. F Whitaker, R. Sobolewski, D. R. Dykaar, T. Y. Hsiang, and G. A. Mourou, "Propagation model for ultrafast signals on superconducting dispersive striplines," *IEEE Trans. Microwave Theory Tech* , vol 36, pp. 277–285, 1988.

[4] O. K. Kwon, B. W. Langley, R. F. W. Pease, and M. R. Beasley, "Superconductors as very high-speed system level interconnects," *IEEE Electron Device Lett.*, vol. EDL-8, pp. 582–585, 1987.

[5] D. Dykaar *et al.*, "High-frequency characterization of thin-film Y–Ba–Cu oxide superconducting transmission lines," *Appl. Phys. Lett.*, vol. 52, pp. 1444–1446, 1988.

[6] M. Wintergill, J. Fontanella, C. Andeen, and D. Schuele, "The temperature variation of the dielectric constant of pure CaF_2, SrF_2, BaF_2 and MgO," *J. Appl. Phys.*, vol 129, p. 1561, 1963.

[7] E. V. Lowenstein, D. R. Smith, and R. L. Morgan, *Appl. Opt.*, vol. 12, p. 398, 1973.

[8] J Antula, "Temperature dependence of dielectric constant of Al_2O_3," *Phys Lett.*, vol 25A, p. 308, 1967.

[9] V. B. Braginsky and V I. Panov, "Superconducting resonators on sapphire," *IEEE Trans. Magn.*, vol. MAG-15, p. 30, 1979.

[10] P. H. Fang and W. S. Brower, "Dielectric constant of Cr_2O_3 crystals," *Phys. Rev.*, vol. 129, p. 1561, 1963.

[11] A. Feinberg, thesis, Northeastern University, 1982 (not published); D. W. Liu, C H Perry, and R. P. Ingel, "Infrared spectra in nonstochiometric Yttria-stabilized zirconia mixed crystals at elevated temperatures," *J. Appl. Phys.*, July 15, 1988.

[12] A. C. Anderson, B. Y. Tsaur, J. W. Steinbeck, and M. S. Dilorio, "RF surface resistance of YBCO thin films," MIT Lincoln Laboratory Quarterly Tech. Rep., Mar. 11, 1988

[13] I. M. Buzin, I V. Ivanov, and G. V. Belokopytov, "Dielectric properties of strontium titanate in the microwave range at temperature 4.2–78 K," *Sov. Phys. Solid State*, vol. 18, pp. 813–814, 1976.

[14] R. O. Bell and G. Rupprecht, "Measurements of small dielectric losses in material with a large dielectric constant at microwave frequencies," *IRE Trans. Microwave Theory Tech.*, vol. MTT-9, p. 239, 1961.

[15] B. P. Gorshunov *et al.*, "Submillimeter properties of high-T_c superconductors," *Physica C*, vol. 153/155, p. 667, 1988.

[16] R. L. Sandstrom *et al.*, "Lanthanum gallate substrates for epitaxial high-T_c superconducting thin films," *Appl. Phys. Lett.*, vol. 53, p. 1874, 1988.

[17] S. Sridhar, C. A. Shiffman, and H. Hamdeh, *Phys. Rev. B*, vol. 36, p. 2301, 1987.

[18] P. L. Ruben *et al.*, *Phys. Rev. B*, vol. 38, p. 6538, 1988.

[19] G. A. Thomas *et al.*, *Phsy. Rev. Lett.*, vol. 61, p. 1313, 1988

[20] T. Timusk and D B. Tanner, "Infrared properties of high-T_c superconductors," in *The Physical Properties of High-Temperature Superconductors*, D. M. Ginsburg, Ed. Singapore: World Scientific Publishing Co., 1989.

[21] K. C. Gupta, R. Garg and I. J. Bahl, *Microstrip Lines and Slotlines*. Dedham, MA, Artech House, 1979

[22] H. A. Wheeler, "Transmission line properties of parallel strips separated by a dielectric sheet," *IEEE Trans. Microwave Theory Tech.*, vol. MTT-13, pp. 172–185, 1965.

[23] D. M. Ginsburg, "Calculation of the electromagnetic absorption edge in superconducting alloys," *Phys. Rev.*, vol. 151, pp. 241–245, 1966.

[24] G. Rickayzen, *Theory of superconductivity*. New York: Wiley, 1965.

[25] D. C. Mattis and J. Bardeen, "Theory of the anomalous skin effect in normal and superconducting metals," *Phys. Rev.*, vol. 111, pp. 412–417, 1958.

[26] M Tinkham, "Far infrared absorption in superconductors," in *Far Infrared Properties of Solids*, S. S. Mitra and S Nudelman, Eds. New York: Plenum Press, 1970; R. A. Ferrell and R. E. Glover, *Phys. Rev.*, vol. 109, p. 1398, 1958; M. Tinkham and R. A. Ferrell, *Phys. Rev. Lett.*, vol. 2, p. 331, 1959.

[27] W. B. Nowak, "The surface impedance of metals at 24,000 MC/sec," Tech Rep. no. 97, Research Laboratory of Electronics MIT, May 27, 1949.

[28] R. A. Pucel, D. J. Masse, and C. P. Hartwig, "Losses in microstrip," *IEEE Trans. Microwave Theory Tech.*, vol. MTT-16, pp. 342–346, 1968; see also correction in vol. MTT-16, p. 1064, 1968.

[29] M. V. Schneider, "Microstrip lines for microwave integrated circuits," *Bell Syst. Tech. J.*, vol. 48, pp. 1422–1444, 1969.

[30] R. Mittra and T. Itoh, "A new technique for the analysis of the dispersion characteristics of microstrip lines," *IEEE Trans. Microwave Theory Tech.*, vol. MTT-19, pp. 47–56, 1971.

[31] E. Yamashita and K Atsuki, "Analysis of microstrip-like transmission lines by nonuniform discretization of integral equations," *IEEE Trans. Microwave Theory Tech.*, vol MTT-24, pp. 195–200, 1976.

[32] E. J. Denlinger, "A frequency dependent solution for microstrip transmission lines," *IEEE Trans. Microwave Theory Tech.*, vol. MTT-19, pp. 30–39, 1971.

[33] T. Itoh and R. Mittra, "Spectral-domain approach for calculating the dispersion characteristics of microstrip lines," *IEEE Trans. Microwave Theory Tech.*, vol. MTT-21, pp. 496–499, 1973.

[34] E. Yamashita, K. Atsuki, and T. Ueda, "An approximate dispersion formula of microstrip lines for computer-aided design of microwave integrated circuits," *IEEE Trans. Microwave Theory Tech* , vol. MTT-27, pp 1036–1038, 1979

[35] W. J. Getsinger, "Microstrip dispersion model," *IEEE Trans Microwave Theory Tech.*, vol. MTT-21, pp. 34–39, 1973.

[36] M. V. Schneider, "Microstrip dispersion," *IEEE Trans. Microwave Theory Tech.*, vol. MTT-20, pp. 144–146, 1972.

[37] E. Hammerstad and O. Jensen, "Accurate models for microstrip computer-aided design," *IEEE MTT-S Int. Microwave Symp. Dig.*, June 1980, pp. 407–409.

[38] H. A. Atwater, "Tests of microstrip dispersion formulas," *IEEE Trans. Microwave Theory Tech.*, vol 36, pp. 619–621, 1988.

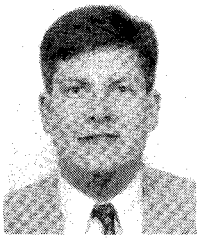

Erik B. Ekholm received the M.Sc. degree in electrical engineering from the Royal Institute of Technology, Stockholm, Sweden, in 1988. His specialization was applied electromagnetics. He studied at Northeastern University on a fellowship from the Royal Institute of Technology in 1987-1988.

Since 1988 he has been employed by McKinsey & Company, Inc., in Scandinavia, and is presently pursuing an MBA at INSEAD in France with a scholarship from McKinsey & Company.

✠

Stephen W. McKnight (M'88) received the B.S. degree in physics from Oberlin College in 1969 and a Ph.D. in experimental solid state physics from the University of Maryland, College Park, in 1977.

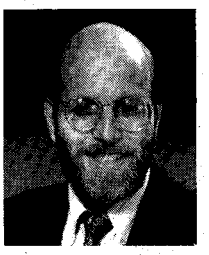

From 1976 to 1978 he was a Research Associate at Emory University, where he worked on the far-infrared properties of A-15 superconductors. In 1978 he was awarded a National Research Council Post-doctoral Fellowship at the Naval Research Laboratory. From 1980 to 1985 he held the position of Assistant Professor in the Department of Physics at Northeastern University and initiated research projects on far-infrared properties of narrow-gap semiconductors under high pressure and on the optical properties of metallic glasses. In 1985 he became a Senior Scientist in the Center for Electromagnetics Research and Adjunct Professor of Electrical Engineering at Northeastern University and in 1988 was appointed Associate Professor of Electrical Engineering. His research in this period has included projects on submillimeter exchange resonance and ferromagnetic resonance of exchange-coupled magnetic multilayers.

Dr. McKnight is a member of the American Physical Society.